The effect of Fe vacancy defects on the physical and electrochemical characterizations of LiFe$_{0.92}$PO$_4$: A combined experimental and theoretical study

Yan Wang [a], Zhe-sheng Feng [a,*], Jing Hu [a], Le Yu [b], Jin-ju Chen [a], Lu-lin Wang [a], Xiao-jun Wang [a], Hai-long Tang [a]

[a] State Key Laboratory of Electronic Thin Films and Integrated Devices, University of Electronic Science and Technology of China, Chengdu 610054, PR China
[b] Catalysis Research Center, Hokkaido University, Sapporo 001-0021, Japan

ARTICLE INFO

ABSTRACT

The LiFe$_{0.92}$PO$_4$ including Fe vacancy defects was prepared as performance-improved cathode material for lithium-ion battery by a carbothermal reduction method. A combination of X-ray diffraction (XRD), Fourier transform infrared spectroscopy (FTIR), X-ray photoelectron spectroscopy (XPS), scanning electron microscope (SEM), transmission electron microscope (TEM), electrochemical testing, and first-principles calculations was used to determine and rationalize the physical and electrochemical characterizations of LiFe$_{0.92}$PO$_4$. The XRD, FTIR and XPS results indicated that Fe vacancy defects had been successfully incorporated into the parent olivine phase of LiFe$_{0.92}$PO$_4$ and did not affect its olivine lattice structure. Especially, the LiFe$_{0.92}$PO$_4$ sample exhibited a discharge capacity of 69.0 mAh g^{-1} at 10 C and capacity retention ratio of 96% after 100 cycles at various rates, implying excellent rate capability and cycling stability. Moreover, the lithium ion migration channels, energy band structures, densities of states, and charge densities of LiFePO$_4$ and LiFe$_{0.92}$PO$_4$ were investigated by first-principles calculations. The results suggest that the higher lithium ion conduction and electronic conductivity of LiFe$_{0.92}$PO$_4$ is attributed to Fe vacancy defects.

© 2013 Elsevier Ltd. All rights reserved.

1. Introduction

Lithium iron phosphate (LiFePO$_4$) is one of the most promising cathode materials for the next-generation of lithium ion battery with high power and energy density due to its high theoretical capacity, environmentally benign, and suitable thermal and chemical stability [1–3]. However, the major issue of LiFePO$_4$ bulk materials is the poor electronic conductivity and low Li-ion diffusion rate [4], which has limited their applications to some extent. Considerable efforts have been made to overcome these drawbacks, such as coating with electronically conducting agents [5,6], cationic doping [7,8], decreasing the particle size [9], and different morphology syntheses [10].

As is well known, vacancy defects within lithium ion battery electrode materials play an important role in lattice structure stability, deformation behavior, elecronic conduction and Li-ion diffusion [11–16]. In recent years, a lot of research work on

the defect chemistry of LiFePO$_4$ has been reported. Masquelier et al. suggested that Fe in the LiFePO$_4$ lattice extrusion generates complex superstructures of the triphylite-type framework for LiFe$_{1-x}$PO$_4$ with air at moderate temperature due to Fe vacancy and possible Li/Fe exchange [11]. Besides, Mauger et al. reported that small magnetic polarons in LiFePO$_4$ were associated with the presence of Fe^{3+} ions introduced by native defects known to be optimized with respect to their electrochemical properties [12]. To have a better understanding of Fe vacancy defects, it is essential to investigate systematically the micro-structural changes and electrochemical performance of LiFe$_x$PO$_4$. However, no combined experimental and theoretical investigations have been carried out to study the effect of Fe vacancy defects on the physical and electrochemical characterizations of LiFe$_x$PO$_4$.

In the present paper, LiFe$_{0.92}$PO$_4$ was prepared by a carbothermal reduction method to produce Fe^{3+} within the lattice and then introduce Fe vacancy defects, which play a vital part in good electronic conductivity and electrochemical performance. In addition, we employed first-principles calculations to study the effect of Fe vacancy defects on the structural and electronic properties of LiFe$_{0.92}$PO$_4$, and gave a mechanism interpretation about how Fe vacancy defects would enhance the electrochemical properties of LiFePO$_4$ material. The results proved theoretically that introduction
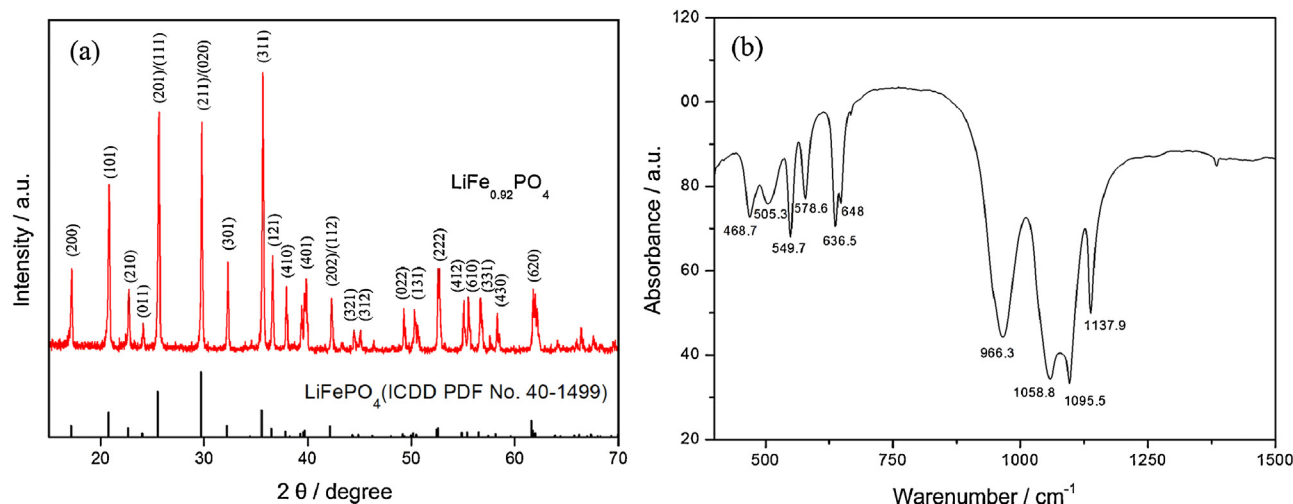
Fig. 1. XRD patterns (a) and FTIR spectra (b) of $LiFe_{0.92}PO_4$.

of Fe vacancy defects is one excellent method to improve electronic and ionic conductivity of $LiFe_{0.92}PO_4$.

2. Experimental

$LiFe_{0.92}PO_4$ was synthesized by carbothermal reduction route as follows. Amounts of LiOH (AR), $(NH_4)_3Fe(C_2O_4)_3 \cdot 3H_2O$ (AR), $NH_4H_2PO_4$ (AR) and acetylene black were dissolved in ethyl alcohol in sequence in the stoichiometric ratio of 1.05: 0.92: 1: 0.38. The suspension was grinded for 10 h using the high energy planetary miller, then the mixed slurry was dried at 60 °C in the oven. After drying, the precursor powder was calcined under flowing N_2 atmosphere at 200 °C for 4 h, followed by sintering at 300 °C for 3 h and 700 °C for 12 h. The heating rate was 6 °C min^{-1}. After cooling to room temperature, the $LiFe_{0.92}PO_4$ was obtained. For electrochemical performance comparison, stoichiometric $LiFePO_4$ was synthesized by the same way.

X-ray diffraction (XRD) pattern was progressed on a SHIMADZU XRD-7000 X-ray diffractometer equipped with Cu Kα radiation. The Fourier transform infrared (FTIR) spectrum of the $LiFe_{0.92}PO_4$ was recorded on a Bruker VERTEX 70 Fourier-transform spectrometer at a spectral resolution of 1 cm^{-1}. X-ray photoelectron spectroscopy (XPS) was obtained using an EASY ESCA instrument with monochromatic Al X-ray radiation (1486.6 eV). A JEOL JSM-7600F was employed to obtain the field-emission scanning electron microscope (SEM) image of the $LiFe_{0.92}PO_4$. A JEOL JEM-100CX analytical equipment was used to get the transmission electron microscope (TEM) image of the sample. Electronic conductivity measurements were performed by four-point probe method using a RTS-9 Digital Instrument. The content of Fe and Li were investigated by inductively coupled plasma-optical emission spectrometer (ICP-OES, SPECTRO ARCOS). The Mössbauer spectrum of the 57 Fe in the sample was obtained on α-Fe foil at room temperature by a Mössbauer spectrometer (Laboratory Equipment Co.).

Electrochemical measurements were performed in two-electrode coin cells (CR-2032) with lithium metal as counter electrode. The working electrode consisted of active material, acetylene black, and polyvinylidene fluoride (PVDF) binder in a weight ratio of 8: 1: 1 was pasted onto aluminum foil and dried at 120 °C in a vacuum oven. The electrolyte used in the measurement was composed of 1 M $LiPF_6$ solution in ethylene carbonate/diethyl carbonate/dimethyl carbonate (1:1:1 by volume). A Celgard 2600 membrane was used as a separator. The cells were assembled in an argon- filled glovebox. Galvanostatic charge-discharge tests were

performed at different current densities between 2.2 and 4.2 V (vs. Li^+/Li) using a EWARE BST-8 electrochemical test instrument.

2.1. Theoretical calculations

The present calculations were carried out based on the density functional theory (DFT) and pseudopotential methods, which were implemented in the first principles calculation program Cambridge Serial Total Energy Package (CASTEP) code. The electronic exchange correlation energy was treated under the generalized gradient approximation (GGA) with the Perdew Burke Ernzerhof method. The experimental geometry of $LiFe_{11/12}PO_4$ was adopted as a model to simulate the $LiFe_{0.92}PO_4$ due to the restriction of the computational resources. Pure bulk olivine-type $LiFePO_4$ has an orthorhombic unit cell, which accommodates 4 $LiFePO_4$ formula units including 28 atoms in all. The possible Fe vacancy defects were simulated by removing a single Fe atom in an 84-atom $LiFePO_4$ supercell with $1 \times 3 \times 1$ repetition. Convergence testing was performed by the $2 \times 1 \times 5$ k-point mesh and 1×10^{-5} eV/atom for total energy tolerance. A cut-off energy of 340.0 eV was used for the plane wave basis expansion [17–21].

3. Results and discussion

The chemical structures of $LiFe_{0.92}PO_4$ were characterized by powder X-ray diffraction analysis. As shown in Fig. 1 (a), the well-resolved diffraction peaks in 15-70° range of 2θ correspond to different crystal planes of $LiFePO_4$ with olivine structure indexed in Pnmb of orthorhombic system (ICDD PDF No. 40-1499). Although iron (III) salt $(NH_4)_3Fe(C_2O_4)_3 \cdot 3H_2O$ was used as the iron source, no peaks were attiributed by usual impurity such as Li_3PO_4, $Li_3Fe_2(PO_4)_3$, and Fe_2O_3. The obtained lattice parameters of $LiFe_{0.92}PO_4$ were a = 6.004 Å, b = 10.315 Å, and c = 4.672 Å, which was similar to the previous reports [22,23]. The structure of $LiFe_{0.92}PO_4$ at the molecular size scale was investigated by FTIR absorption experiments and was shown in Fig. 1 (b). IR bands of $LiFePO_4$ have been already identified and discussed in earlier works [24,25]. As we can see in the FTIR spectra, there is not much difference in the vibrational modes (region 400-1500 cm^{-1}) of usual $LiFePO_4$. Bands of the bending vibration of PO_4^{3-} anion were located at 468.7, 505.3, 549.7, 578.6 and 636.5 cm^{-1}, while the peaks at 966.3, 1058.8, 1095.5 and 1137.9 cm^{-1} were assigned to stretching vibration of PO_4^{3-}. No peaks of possible impurity phases such as Fe_2O_3, $FePO_4$, and Li_3PO_4 were observed in FTIR spectrum. Combining with XRD and FTIR, it can be indicated that